Colloidal Nanostructures of Transition Metal Dichalcogenides

Yifan Sun,[1,5,†] Mauricio Terrones,[1,2,3,5,*] and Raymond E. Schaak[1,4,6,*]

[1] Department of Chemistry, [2] Department of Physics, [3] Department of Materials Science and Engineering, [4] Department of Chemical Engineering, [5] Center for 2-Dimensional and Layered Materials, and [6] Materials Research Institute, The Pennsylvania State University, University Park, Pennsylvania 16802, USA.

Present Address: [†]Chemical Sciences Division, Oak Ridge National Laboratory, Oak Ridge, Tennessee 37831, USA.

Corresponding authors: mut11@psu.edu (M.T.); res20@psu.edu (R.E.S.)

CONSPECTUS

Layered transition metal dichalcogenides (TMDs) are intriguing two-dimensional (2D) compounds where metal and chalcogen atoms are covalently bonded in each monolayer, and the monolayers are held together by weak van der Waals forces. Distinct from graphene, which is chemically inert, layered TMDs exhibit a wide range of electronic, optical, catalytic, and magnetic properties dependent upon their compositions, crystal structures, and thicknesses, which make them fundamentally and technologically important. TMD nanostructures are traditionally synthesized using gas-phase chemical deposition methods, which are typically limited to small-scale samples of substrate-bound planar materials. Colloidal synthesis has emerged as an alternative synthetic approach to enable the scalable synthesis of free-standing TMDs. Judicious selection of precursors, solvents, and capping ligands, together with optimization of synthetic parameters such as concentrations and temperatures, leads to the fabrication of colloidal TMD nanostructures exhibiting tunable properties. In addition, understanding the formation and transformation of TMD nanostructures in solution contributes to the discovery of important structure–function relationships, which may be extendable to other anisotropic systems.

In this Account, we summarize recent progress in the colloidal synthesis, characterization, and applications of TMD nanostructures with tunable compositions, structures, and thicknesses. Based on the preparation of Mo- and W-based disulfide, diselenide, and ditelluride nanostructures, we discuss examples of phase engineering, where various metastable TMD compounds can be directly accessed at low temperatures in solution. We also analyze the chemistry involved in broadly tuning composition across the $MoSe_2$–WSe_2, WS_2–WSe_2, and $MoTe_2$–WTe_2 solid solutions, as well as atomic-level microscopic characterization and the resulting composition-tunable properties. We then highlight how the high densities of defects in the colloidally synthesized TMD nanostructures enable unique catalytic properties, including their ability to facilitate the selective hydrogenation of substituted nitroarenes using molecular hydrogen. Finally, using this library of colloidal TMD nanostructures as substrates, we discuss the pathways by which noble metals deposit onto them in solution. We highlight the importance of the relative strengths of the interfacial metal–chalcogen bonds in determining the sizes and morphologies of the deposited noble metal components. These synthetic capabilities for colloidal TMD nanostructures, which have been generalized to a library of composition-tunable phases, enable new systematic studies of structure-property relationships and chemical reactivity in this important class of 2-D materials.

KEY REFERENCES

- Sun, Y.; Wang, Y.; Sun, D.; Carvalho, B. R.; Read, C. G.; Lee, C.; Lin, Z.; Fujisawa, K.; Robinson, J. A.; Crespi, V. H.; Terrones, M.; Schaak, R. E. Low-temperature solution synthesis of few-layer 1T′-$MoTe_2$ nanostructures exhibiting lattice compression. *Angew. Chem. Int. Ed.* **2016**, *55*, 2830–2834.[1] *Demonstrates the ability to directly synthesize a metastable colloidal transition metal ditelluride using low-temperature solution methods.*

- Sun, Y.; Fujisawa, K.; Lin, Z.; Lei, Y.; Mondschein, J. S.; Terrones, M.; Schaak, R. E. Low-temperature solution synthesis of transition metal dichalcogenide alloys with tunable optical properties. *J. Am. Chem. Soc.* **2017**, *139*, 11096–11105.[2] *Defines a library of synthetically-accessible colloidal TMD solid-solution nanoparticles, provides atomic-scale microscopic insights into local structure and composition, and investigates their composition-dependent optical properties.*

- Sun, Y.; Darling, A. J.; Li, Y.; Fujisawa, K.; Holder, C. F.; Liu, H.; Janik, M. J.; Terrones, M.; Schaak, R. E. Defect-mediated selective hydrogenation of nitroarenes on nanostructured WS_2. *Chem. Sci.* **2019**, *10*, 10310–10317.[3] *Reveals how sulfur vacancies on the basal planes and tungsten-terminated edges of colloidal WS_2 nanostructures facilitates the selective hydrogenation of substituted nitroarenes using molecular hydrogen.*

- Sun, Y.; Wang, Y.; Chen, J. Y. C.; Fujisawa, K.; Holder, C. F.; Miller, J. T.; Crespi, V. H.; Terrones, M.; Schaak, R. E. Interface-mediated noble metal deposition on transition metal dichalcogenide nanostructures. *Nat. Chem.* **2020**, *12*, 284–293.[4] *Elucidates the pathways by which noble metals deposit on various colloidal TMDs, including the important role of interfacial bonding when coupling TMDs with noble metals.*

1. INTRODUCTION

Layered transition metal dichalcogenides (TMDs) are important two-dimensional (2D) nanomaterials that have unique thickness-dependent properties, a rich phase diagram spanning a variety of compositions and crystal structures, and a wide range of different chemical and physical properties that make them attractive candidates for many potential applications.[5,6] Accessing these properties, which is a prerequisite to enabling their applications, requires the ability to precisely control their thicknesses, compositions, crystalline phase, and surface chemistry, as well as vacancies and other types of defects. Once these features are controlled, 2D TMDs also become powerful platforms for fundamental studies of interlayer coupling, phase engineering, charge transfer, and interfacial phenomena.[7,8]

TMD nanostructures are typically synthesized using gas-phase chemical deposition methods, which involve reacting substrate-confined metal precursors with chalcogen reagents at elevated temperatures. While the gas-phase approaches produce high-quality TMD monolayers that are ideal for exploring new quantum phenomena and demonstrating high-performance devices,[5] the low yields, substrate confinement, and harsh synthetic conditions limit aspects of their scalability, as well as their scope of applications. Solution routes to TMD nanostructures have emerged as an alternative synthetic approach that addresses several of these disadvantages,

including scalability and the production of TMDs that are not bound to a substrate.[9,10] Solution-based inorganic nanoparticle synthesis methods generally work by thermally or chemically transforming solubilized reagents into colloidal nanostructures stabilized by surface capping ligands. These approaches routinely produce high-quality quantum dots and noble metal nanoparticles, which are widely applied in optical, biomedical, and catalytic applications.[11,12] For TMD systems, careful control over the reaction parameters can produce 2D TMD nanosheets with adjustable lateral sizes and thicknesses for tunable light emission, as well as 3D nanoflower-like aggregates with high surface areas that are ideal for catalysis. For example, colloidal WS_2 monolayer quantum dots have been used to study how different solvents influence photoluminescence energy and intensity,[13] while colloidal WS_2 nanoflowers with intrinsic sulfur vacancies were found to be active catalysts for the selective hydrogenation of substituted nitroarenes.[3] In the colloidal synthesis of group IV TMDs that include ZrS_2, TiS_2 and HfS_2, continuous influx of chalcogen reagents can promote lateral growth to yield single-layer nanosheets, while more reactive reagents that have a burst influx early in the reaction tend to form multilayer nanosheets.[14] Meanwhile, individual TMD layers have a strong tendency to aggregate, which can produce nanoflowers in colloidal systems; surface capping ligands can help to modify the inter-nanosheet interactions, resulting in different degrees of aggregation.[15]

The formation of TMD nanostructures in solution is typically triggered by the decomposition of metal and chalcogen precursors to monomer complexes, followed by their reaction to form small nuclei protected by long-chain organic ligands upon heating.[16] The nuclei then grow to form nanocrystals through a process that is highly tunable. Judicious choice of precursor and solvent permits modulation of the surface energy of the exposed facets, promoting either lateral growth of 2D nanosheets or vertical growth of TMD layers to form thicker sheets.

Colloidal synthesis routes to some of the most highly-studied transition metal disulfides and diselenides have been reported, but analogous capabilities for transition metal ditellurides had not been reported. Additionally, broad composition tunability, which exists for gas-phase routes to substrate-bound TMDs,[17] had not been demonstrated for colloidal systems. The scope of TMDs available as colloidal nanostructures lagged behind that of substrate-bound systems. For example, because the properties of TMDs depend on their crystal structures, the ability to control the phase that is formed – for example the 1T (or 1T′) *vs*. 2H *vs*. T_d polymorphs – would allow colloidally synthesized TMDs to have potentially expanded capabilities for optoelectronics, catalysis, and magnetism.[18] Subtle differences in metal–chalcogen coordination environments, types and locations of atomic vacancies, and various stacking faults can also contribute significantly to the properties of TMDs, but they can be challenging to characterize, especially for colloidal systems.

In this Account, we highlight recent progress in the colloidal synthesis and applications of mono- and few-layer TMD nanostructures and their derivatives, as well as important insights gained from in-depth characterization. We focus on the TMD tellurides $MoTe_2$ and WTe_2, as well as the $MoSe_2$–WSe_2, WS_2–WSe_2, and $MoTe_2$–WTe_2 solid solutions that possess widely tunable compositions. We also highlight the use of colloidal TMDs as catalysts for selective hydrogenation reactions, which are of interest to organic chemists.[19] We further demonstrate the use of this library of colloidal TMD nanostructures as substrates for noble metal deposition in solution, which leads to the formation of various TMD–nanoparticle composites including systems where atomically thin films of noble metals decorate the surfaces of colloidal TMD nanostructures. Across all of these examples, we highlight unique insights into structure, composition, defects, and interfaces that emerge from in-depth characterization through microscopy, spectroscopy, and diffraction, as well as theoretical calculations. These results are organized into four topics based on their chemistry: (1) targeting phases, (2) programming

composition, (3) engineering defects, and (4) constructing heterostructures. Together, these capabilities provide potential new opportunities for predicting and rationally designing complex TMD nanostructures with targeted properties and new applications.

2. TARGETING PHASES

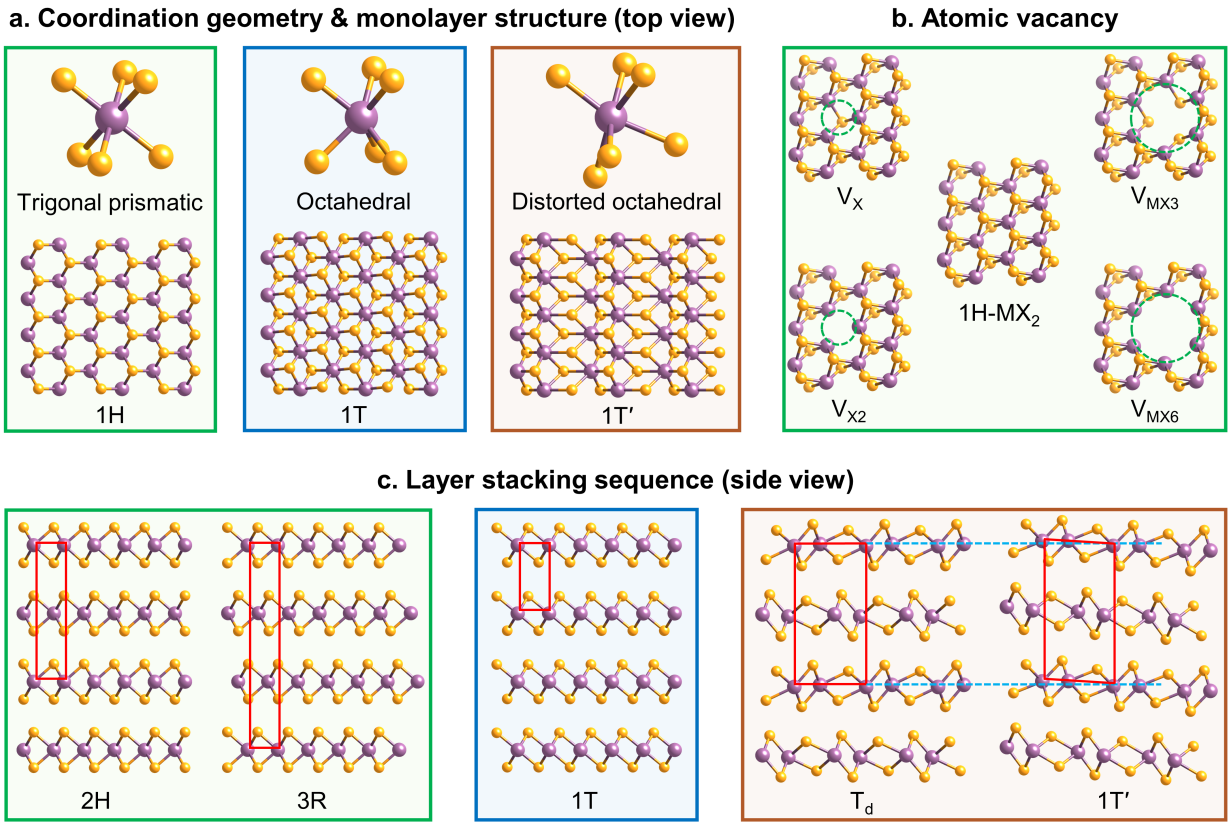

Figure 1. Schematic showing the structures of layered TMDs. (a) Coordination geometries and corresponding monolayer structures (top view). Metal (M) and chalcogen (X) atoms are in purple and orange, respectively. (b) Pristine structure (center) and different types of vacancies (dashed green circles) in monolayer 1H-MX_2. (c) Multilayer structures (side view) of layered TMDs. Unit cells are outlined in red, and the dashed blue lines highlight the subtle differences between the T_d and 1T′ structures.

The most commonly studied TMDs – which include the disulfides, diselenides, and ditellurides of molybdenum and tungsten – adopt one of several structurally related polymorphs, and multiple crystal structures that differ only subtly, may be accessible for the same elemental composition. Controllably synthesizing one particular crystal structure for a given composition can therefore be challenging. As illustrated in Fig. 1, the two phases that are most commonly observed for TMDs are the 2H phase with trigonal prismatic coordination and the 1T phase (mostly observed as a distorted 1T′ phase) with octahedral coordination.[5,20] Another less-commonly reported orthorhombic (T_d) phase is similar to 1T′, except that the layers are directly stacked in a higher-symmetry manner. This rich polymorphism leads to phase-specific properties and applications. For example, 2H-type TMDs, which are semiconducting, function as

highly efficient photocatalysts.[21] 1T-type TMDs, which are metallic or semimetallic, offer improved performance as hydrogen evolution catalysts and supercapacitor electrodes due to decreased barriers to charge transfer.[22,23] For bulk $MoTe_2$, superconductivity is observed for the T_d phase, but not for the 1T′ or 2H phases.[24]

Many of these TMD polymorphs are thermodynamically favorable only at high temperatures,[25] which makes them difficult to synthesize in a targeted way as colloidal nanostructures in solution, which generally has an upper limit of ~ 300 ºC. However, ligand and solvent molecules bind to the surfaces of colloidal TMDs, which modulates their energetics, since they are 2D materials that consist mostly of exposed surfaces in solution. As a result, solution routes to TMD nanostructures offer a unique platform for targeting desired TMD phases while also controlling nanostructural features and exposed surface areas. In a pioneering study, Mahler *et al.* achieved phase engineering of WS_2 as colloidal nanosheets (Fig. 2a).[21] Here, the 2H-WS_2 and 1T-WS_2 polymorphs were selectively synthesized by including or excluding hexamethyldisilazane (HMDS). During the synthesis, HMDS functions as a coordinating ligand that modifies the geometry and reactivity of the metal precursor, which contributes to the crystallization and phase tuning of metal chalcogenide nanocrystals.[26] The presence or absence of HMDS as a surface-capping ligand functionalizing the as-formed TMD monolayers also results in distinct reaction pathways that ultimately produce different morphologies. 1T-WS_2 nanosheets, which have strong electrostatic surface interactions, are stabilized as individual monolayers while 2H-WS_2 nanosheets, which have weak surface interactions, tend to aggregate to form nanoflowers. A study from Sokolikova *et al.* further expanded this phase targeting capability to 1T′-WSe_2, which exhibits enhanced electrocatalytic activity for the hydrogen evolution reaction (HER) relative to its 2H counterpart.[27]

The ability to target metastable 1T (or 1T′) phases of colloidal transition metal disulfides and diselenides using solution-based reactions is now well established. Expanding these phase targeting capabilities to ditellurides such as $MoTe_2$ and WTe_2 is important because they exhibit unique properties relative to their disulfide and diselenide cogeners.[28–30] However, synthetically, this is challenging to achieve, given the different reactivity of telluride reagents relative to sulfide and selenide reagents, as well as the greater surface oxidation tendency and thermal instability of the ditellurides.

To target the synthesis of $MoTe_2$, we injected a molybdenum(V) oleate precursor dropwise into a mixture of trioctylphosphine (TOP), trioctylphosphine telluride (TOP-Te), oleylamine, and HMDS at 300 ºC.[1] TOP prevents the precipitation of elemental Te due to P=Te bond formation at elevated temperatures,[31] and oleylamine provides a reducing atmosphere that facilitates the transformation from Mo(V) to Mo(IV), while also functioning as a surface capping ligand that mitigates surface oxidation of the colloidal ditellurides.[32] As shown in Fig. 2b, the product had a flower-like morphology that contained few-layer $MoTe_2$ nanosheets protruding out in all directions from a central core. We initially thought that 2H-$MoTe_2$ would form, as that is the thermodynamically preferred polymorph (in bulk systems) at 300 ºC. However, the nanoflowers instead adopted the metastable 1T′-$MoTe_2$ structure.[1] Density functional theory (DFT) calculations provided important insights into the formation and stability of 1T′-$MoTe_2$. The calculated energy difference between 1T′- and 2H-$MoTe_2$ is much smaller than the energy difference between the 1T′ and 2H phases for MoS_2 and $MoSe_2$, rendering both phases potentially accessible at low or moderate temperatures and therefore helping to rationalize how 1T′-$MoTe_2$ could form. The unique flower-like morphology also helps to stabilize the 1T′-$MoTe_2$ polymorph. The 1T′-$MoTe_2$ nanosheets that comprise the nanoflowers are polycrystalline with small, 5-10 nm domains. To undergo a phase transition from 1T′-$MoTe_2$ to 2H-$MoTe_2$, *i.e.* a transformation from the metastable to the stable polymorph, would require a simultaneous

change in both the *a* and *b* lattice parameters (i.e. in two crystallographic directions), which is disfavored because the grain boundaries that connect the small 5-10 nm domains effectively pin the structure and prevent it from expanding laterally. The 1T′-$MoTe_2$ polymorph is therefore stabilized.

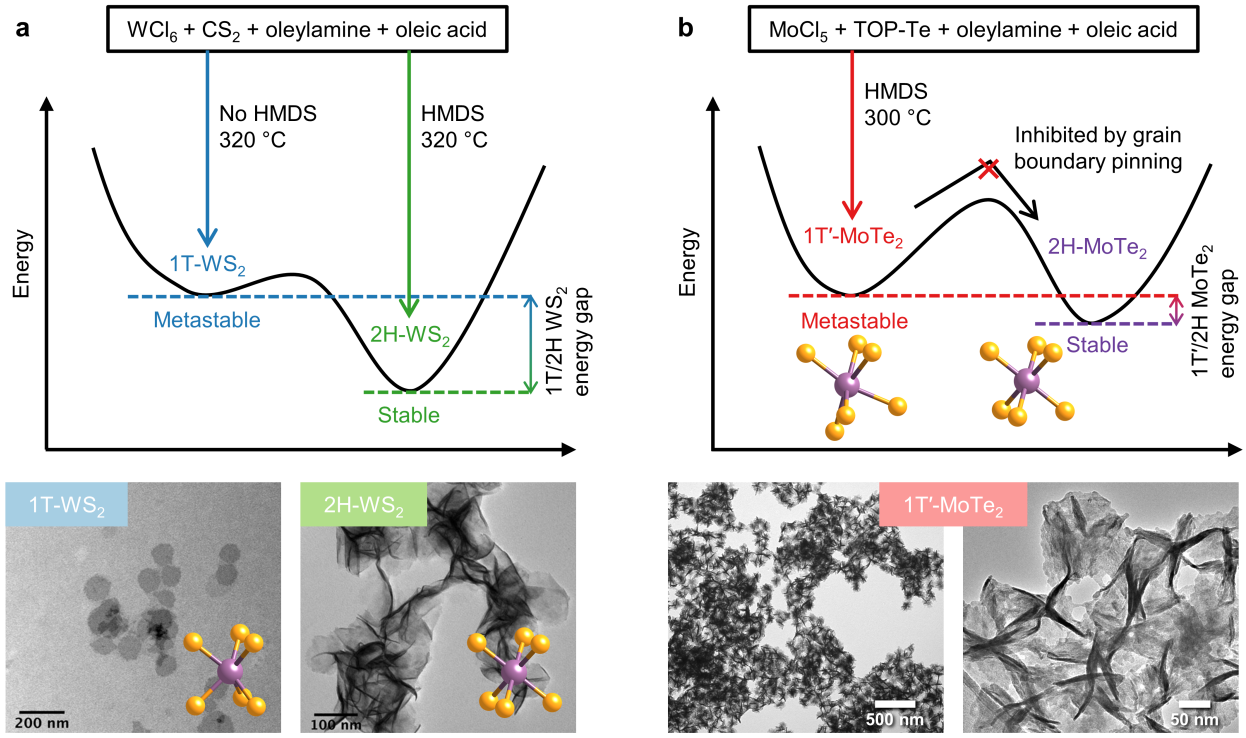

Figure 2. (a) Schematic illustrating the selective formation of the metastable 1T-WS_2 and the stable 2H-WS_2 phases by including and excluding HMDS. The TEM images were adapted with permission from ref. 21. Copyright 2014 American Chemical Society. (b) Schematic illustrating the formation of the metastable 1T′-$MoTe_2$ nanostructures, which are further stabilized against conversion to the stable 2H phase through grain boundary pinning. The TEM images were adapted with permission from ref. 1. Copyright 2016 John Wiley & Sons, Inc.

We further prepared few-layer WTe_2 nanostructures using a similar approach, where tungsten oleate was injected dropwise into a solution containing oleylamine, TOP-Te, and HMDS at 300 ºC.[33] Aliquot studies suggested that 2D WTe_2 nanosheets formed rapidly during the hot-injection synthesis, followed by simultaneous lateral and vertical growth processes that ultimately led to the formation of a nanoflower-like morphology. Atomic-resolution microscopic images capture the curvature-induced displacement of the relative positions of tungsten and tellurium atoms in the monolayer region of the WTe_2 nanoflowers (Fig. 3). Interestingly, we observed a co-existence of 2H and 2H′ stacking sequences for some of the neighboring WTe_2 bilayers,[34] which demonstrates the atomic-level complexity and diversity of local TMD structures. The colloidal 1T′-$MoTe_2$ and WTe_2 nanostructures tend to oxidize significantly upon exposure to air, thus requiring storage under inert atmospheres.

Besides formation and stabilization of the metastable TMD phases, the solution environment can also aid in facilitating phase transformations. For example, lithiation and subsequent exfoliation of bulk crystals can yield mono- to few-layer TMD nanosheets having the metallic 1T′ phase.[35] Recovery back to the semiconducting 2H phase typically requires high-temperature treatment, where the exfoliated nanosheets must be transferred to solid substrates to avoid

aggregation. Through surface functionalization, chemically exfoliated MoS_2 and WS_2 nanosheets are readily transferred to non-polar solvents with high boiling points, and further solution-phase annealing enables efficient conversion of the metallic 1T′ phases to the semiconducting 2H phases.[36] Moreover, the annealed TMD nanosheets exhibit minimal surface oxygenation and aggregation due to the protection afforded by the surface-capped ligands. This process synergistically combines the scalability of chemical exfoliation with ease of solution processing, demonstrating a new strategy to manufacture transferrable free-standing TMD nanosheets that can be further integrated in a broad scope of device applications.[37] More studies on the surface functionalization of colloidal TMDs will enable new understanding of charge transfer across the TMD/molecule interface and the ability to tune the corresponding optical properties.[13]

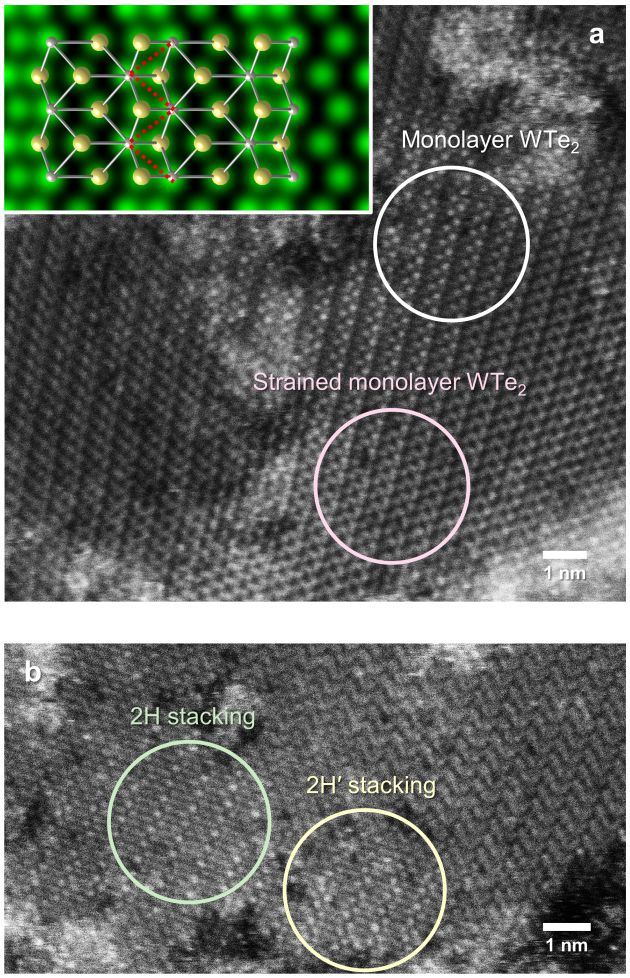

Figure 3. (a) High-resolution ADF-STEM image for the WTe_2 nanostructures. The monolayer region highlighted by the white circle matches well with the simulated zig-zag pattern marked with red dotted lines in the inset. Surface strain is evident by the transformation from the zig-zag pattern to the parallel one (pink circle), consistent with the flower-like morphology. (b) 2H- and 2H′-analogous stacking of WTe_2 layers, highlighted by light green and light yellow circles, respectively. Adapted with permission from ref. 33. Copyright 2017 The Royal Society of Chemistry.

3. PROGRAMMING COMPOSITION

In addition to targeting phases and tuning dimensionality, programming composition is another synthetic lever for achieving tunable properties in nanostructured TMDs. The metal or chalcogen atoms in a parent TMD compound can be substituted with other metal or chalcogen atoms to form a solid-solution product having a continuously variable composition that can be continuously fine-tuned to achieve targeted properties for catalytic, optoelectronic, and topological devices.[38] Fully composition-tunable solid solutions that span the $MoSe_2$–WSe_2 ($Mo_xW_{1-x}Se_2$) and WS_2–WSe_2 ($WS_{2y}Se_{2(1-y)}$) solid solutions were synthesized as colloidal nanoflowers, analogous to the $MoTe_2$ and WTe_2 systems described above.[2] The TMD metal alloys, $Mo_xW_{1-x}Se_2$, were directly synthesized by the dropwise injection of stoichiometric amounts of $MoCl_5$ and WCl_6 in oleic acid into a solution of oleylamine, HMDS, and diphenyl diselenide at 300 ºC. Accessing the chalcogen alloys, $WS_{2y}Se_{2(1-y)}$, requires careful consideration of reagent activity, since sulfur tends to rapidly evaporate and/or decompose at elevated temperatures before reacting with the tungsten precursor. Therefore, in contrast to the synthesis of $Mo_xW_{1-x}Se_2$ that used stoichiometric metal reagents, diphenyl diselenide was added to the CS_2-based protocol for WS_2 to access sulfur-rich alloys ($WS_{2y}Se_{2(1-y)}$; y = 1, 0.81, 0.70, 0.60)[21], while diphenyl disulfide, which exhibits a higher utilization compared with that of CS_2, was added to the WSe_2 end member to prepare selenium-rich alloys ($WS_{2y}Se_{2(1-y)}$; y = 0.44, 0.13, 0.06, 0).

Confirming the formation of composition-tunable solid solutions, and understanding how the atoms are mixed at the atomic level, can be challenging for colloidal TMD nanostructures. Bulk characterization techniques, including X-ray diffraction (XRD) and Raman spectroscopy, provide structural information, including confirmation of a particular polymorph and evidence of composition modulation. However, the polycrystallinity, small domain sizes, and strain within the nanosheets that comprise the colloidal TMD nanostructures result in broad XRD peaks.[39] Advances in electron microcopy in the past few decades have led to atomic-level understanding of atom distributions into 2D TMD nanosheets.[40] The nanosheets that comprise the colloidal TMD nanostructures, however, tend to curl and not lay flat on the TEM grid. This complicates TEM analysis and makes it difficult to differentiate between atomically-mixed alloys vs. more segregated structures composed of nanoscale patches that are connected through grain boundaries.

To gain atomic-level composition insights into the colloidal TMD nanostructures, the electron microscopy tools that are commonly applied to 2D TMD nanosheets were combined with tilt-angle-dependent analyses to compensate for off-axis effects. As displayed in Fig. 4, annular dark field–scanning transmission electron microscopy (ADF-STEM) imaging allows differentiation of atomic configurations based on the Z-contrast, *i.e.* atomic number. ADF-STEM imaging reveals a random distribution of the alloyed metal or chalcogen elements, corroborating the formation of true alloys at the atomic scale in the colloidal nanostructures. Various types of point vacancy sites, including metal vacancies (V_{Mo} and V_W), mono-chalcogen vacancies (V_S and V_{Se}), and di-chalcogen vacancies (V_{S2} and V_{Se2}), were also identified by comparison with simulated ADF images, indicating that the colloidal TMD nanosheets are defect-rich. A tilt-angle dependence of the intensities associated with ADF imaging line scans was also observed for the curled TMD nanosheets, providing atomic-level insights into the structures of colloidal TMD alloys. This is important, because such atomic-level insights had previously only been available for planar TMD nanosheets synthesized on a substrate through chemical or vapor deposition, not synthesized in solution as colloidal TMD nanostructures.

UV-vis adsorption spectra show that the A excitonic transition of the colloidal $Mo_xW_{1-x}Se_2$ and $WS_{2y}Se_{2(1-y)}$ nanostructures can be readily tuned between 1.51 and 1.93 eV through metal and chalcogen alloying, further correlating atomic structure engineering with modification of the optical properties (Fig. 5). This method could also potentially be applied to the synthesis of more complex ternary and quaternary TMD alloys. Ordered TMD alloys or superlattices, which have been computationally predicted to have a small energetic preference relative to random substitutional alloys,[41] may also be accessible with colloidal synthesis, as atom migration could be better inhibited at the relatively low temperatures of solution synthesis compared to higher-temperature gas-phase synthesis.

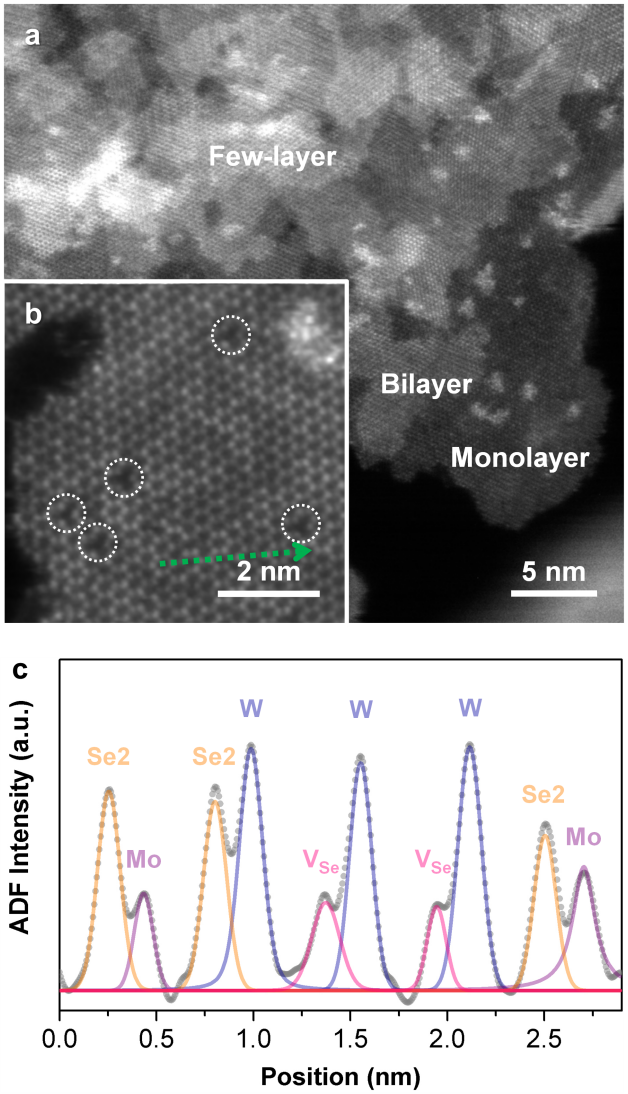

Figure 4. (a) High-resolution ADF-STEM image highlighting a region of the $Mo_{0.35}W_{0.65}Se_2$ nanostructures, showing few-layer, bilayer, and monolayer regions. (b) Atomically resolved ADF-STEM image of the $Mo_{0.35}W_{0.65}Se_2$ nanostructures, where chalcogen vacancies are highlighted in white circles. (c) Experimental ADF intensity curve (gray) corresponding to the line scan indicated by the green arrow in (b), where the atomic configurations are identified based on the simulated profiles (colored). Adapted with permission from ref. 2. Copyright 2017 American Chemical Society.

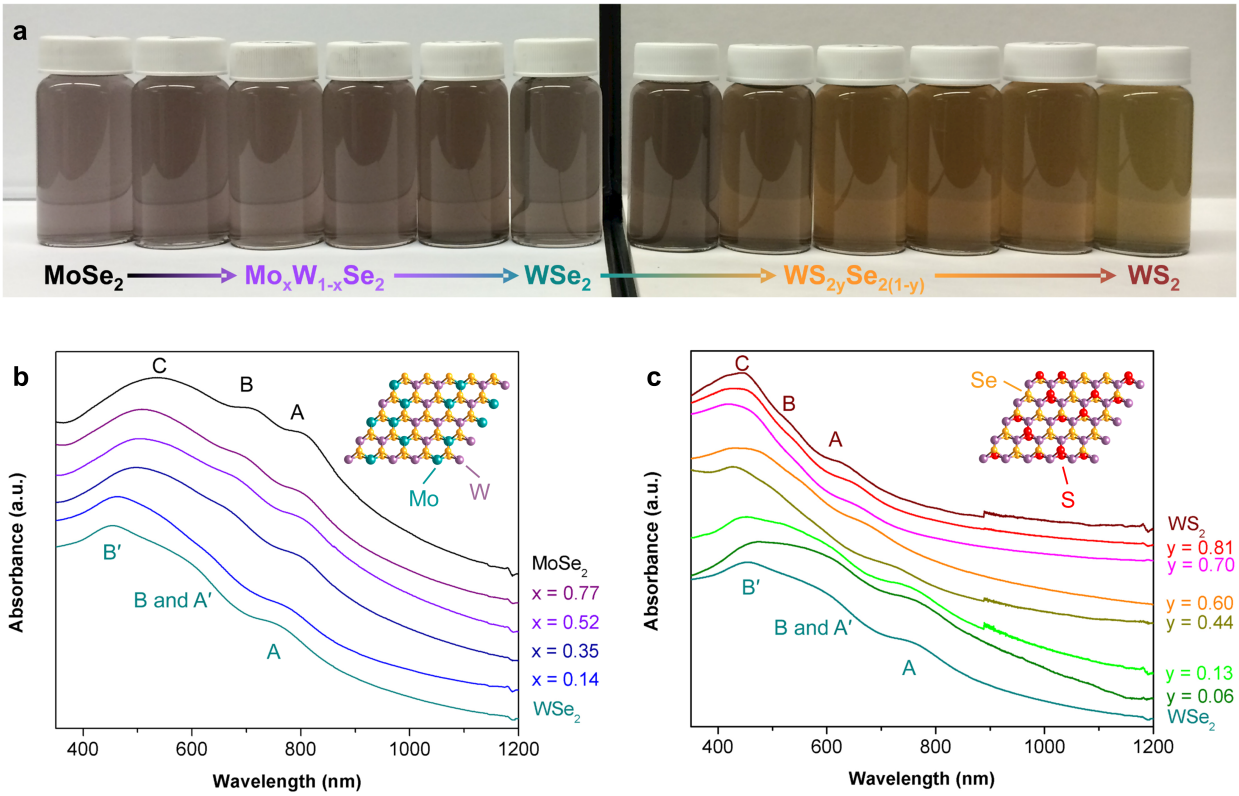

Figure 5. (a) Photograph of metal ($Mo_xW_{1-x}Se_2$) and chalcogen ($WS_{2y}Se_{2(1-y)}$) alloy samples dispersed in ethanol. UV−vis absorbance spectra of (b) $Mo_xW_{1-x}Se_2$ and (c) $WS_{2y}Se_{2(1-y)}$, along with schematic showing the random distribution of metal (W & Mo) and chalcogen (S & Se) atoms. Adapted with permission from ref. 2. Copyright 2017 American Chemical Society.

4. ENGINEERING DEFECTS

Most computational predictions of the properties of TMDs, as well as rationale provided for experimental measurements, are based on “perfect” ideal models. However, increasing discrepancies between theoretical investigations and experimental results suggest that structural imperfections play significant roles in modulating the properties of TMD nanosheets.[42] For example, TMD nanosheets typically exhibit p-type or n-type behavior in electronic devices, which is distinct from what would be expected based on perfect compositions and crystal structures.[43] Colloidal TMD nanostructures are synthesized in solution, which involves significantly lower temperatures than are required for gas-phase deposition approaches to the more mainstream substrate-bound TMD nanosheets. In solution, the molecular species that are present during the reaction have the potential to extract chalcogen atoms into organic solvents through the formation of complexes.[31] As a result, the as-synthesized colloidal TMD nanostructures typically have a high density of defects including point atomic vacancies and grain boundaries, as well as metal- or chalcogen-terminated edge sites and stress that is caused by curling and buckling. All of these features can impact the properties in ways that can be either beneficial or detrimental, depending on the specific application. For instance, intrinsic defects significantly lower the electronic device mobility,[44] while significantly improving the electrocatalytic performance for HER.[45] It is therefore important to understand the formation and manipulation of structural defects in colloidal TMD nanostructures, as well as their impact on properties.

Layered transition metal disulfides are predicted to have near-zero free energy of adsorption of molecular hydrogen on the edges and defect sites, making them useful non-platinum group materials that can catalyze the HER.[46] Transition metal disulfides are also used as heterogeneous catalysts for hydrogenation reactions because of their ability to activate hydrogen. As hydrogenation catalysts, transition metal promotors are typically required to increase the catalytic activity through lowering the metal–sulfur bond energy.[47,48] We found that the solution-synthesized colloidal WS_2 nanostructures catalyze hydrogenation reactions without transition metal promotors, where the abundant defects play a key role.[3] The colloidal WS_2 catalyst allows the use of molecular hydrogen to facilitate the selective hydrogenation of substituted nitroarenes to their corresponding aniline derivatives, where the nitro groups are selectively converted to amines while the other reducible functional groups remain unaltered (Fig. 6). Computational studies indicated that the atomic sulfur vacancies on the basal planes and the tungsten-terminated edges, which were also observed microscopically, are the active sites that lead to chemoselectivity. Geometry-confined adsorption and step-wise conversion both favor selective hydrogenation of 3-nitrostyrene to 3-nitroaniline on the defect-rich WS_2 surfaces. These mechanistic insights are useful for achieving targeted catalytic reactions, as well as for developing new materials, such as gas sensors that function based on the interactions between the targeted molecules and the defect-rich TMD surfaces.[49]

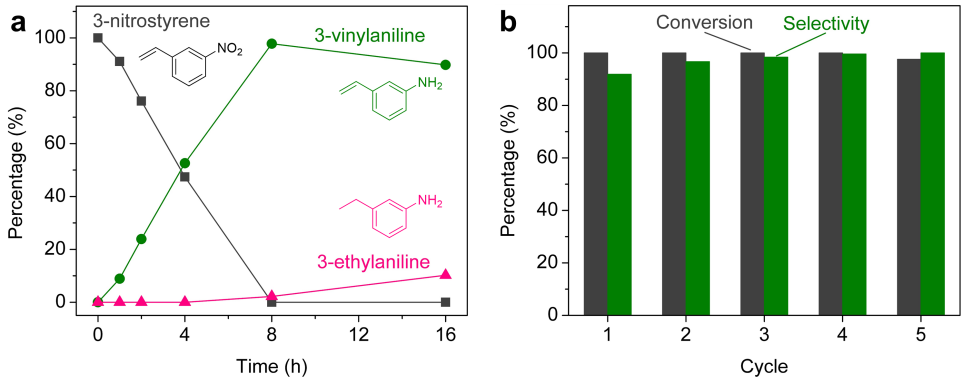

Figure 6. (a) Aliquot study for the selective hydrogenation of 3-nitrostyrene catalyzed by 2H-WS_2 nanostructures, showing the percentage of 3-nitrostyrene (grey), 3-vinylaniline (green), and 3-ethylaniline (pink) at different reaction times. (b) Percent conversion (grey) and selectivity (green) for the hydrogenation of 3-nitrostyrene to 3-vinylaniline using the same nanostructured 2H-WS_2 catalyst over five successive cycles. Reproduced with permission from ref. 3. Copyright 2019 The Royal Society of Chemistry.

Other complementary defect engineering strategies have also been developed. Han *et al.* reacted colloidal 2H-NbS_2 nanosheets, which function as Lewis bases, with $AlCl_3$, which is a Lewis acid, to controllably introduce nanopores in the 2D TMD nanosheets under mild conditions.[50] Initial electrophilic addition leads to the formation of Al–S bonds, which disrupts the bonding in the [Nb–S–Nb] subunits, and further transmetalation and dimerization steps produce $NbCl_5$ and $Al_2SCl_5^-$ that dissolve in solution. This acid-base transformation can be further applied to 1T-TiS_2 with a well-maintained 1T phase, indicating its wide applicability for colloidal TMD nanostructures across a range of polymorphs. Introducing nanopores is advantageous for increasing the surface area of TMDs, which was used to enhance electrochemical capacitance.[23]

5. CONSTRUCTING HETEROSTRUCTURES

Composition-tunable colloidal TMD nanostructures are now accessible, and these are being explored for their unique optical and catalytic properties.[2,3,21,27,51] Meanwhile, this diverse library of TMD nanostructures, having identical nanoflower-like morphologies, is also fundamentally useful for understanding how to deposit other materials onto them. Such capabilities are important for connecting TMDs to other materials and for creating new synergistic functions that could emerge from the interfaces between them.[52] The deposition of noble metals, such as Au and Ag, is especially important. TMDs are known to electronically modify deposited metals, influencing their catalytic properties.[53] The deposition of Au and Ag onto TMDs would also be important for making electrical contact to them for device integration.[54] However, controlling noble metal deposition onto TMDs, and understanding how and why the TMD–metal interfaces form, is challenging. From a synthetic perspective, morphologically equivalent TMD nanostructures that span a wide range of compositions and structures, which are important for useful comparisons, have previously been difficult to generate.[17]

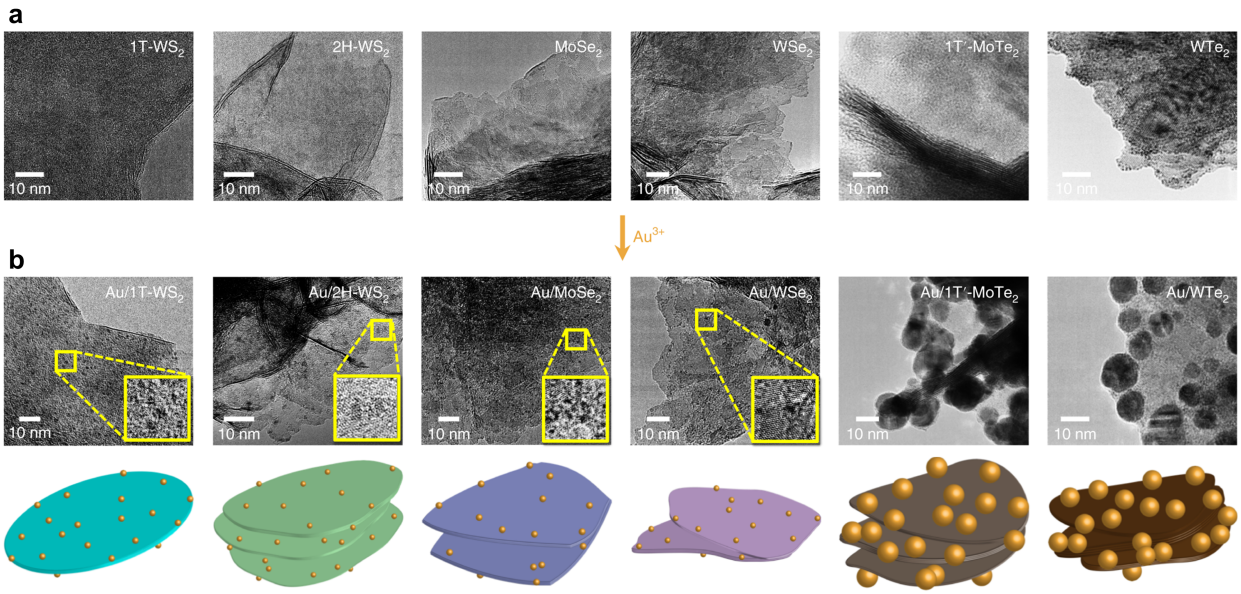

Figure 7. TEM images of each type of the colloidal TMD nanostructures (a) before and (b) after the reaction with Au^{3+}, which produces gold nanoparticles anchored to the TMD nanosheet surfaces. Drawings below the TEM images highlight the key features of each system. Adapted with permission from ref. 4. Copyright 2020 Nature Publishing Group.

Using our library of colloidal TMD nanostructures, we investigated the solution-phase seeded growth of Au and Ag onto colloidal 1T-WS_2, 2H-WS_2, 2H-$MoSe_2$, 2H-WSe_2, 1T′-$MoTe_2$, and T_d-WTe_2 nanosheets *via* a spontaneous redox reaction between the TMD nanosheet surface and noble metal cations.[4] The deposition of Au onto all six of these colloidal TMD nanostructures produce uniform Au nanoparticles, which together constitute hybrids of zero-dimensional (0D) Au nanoparticles and 2D TMDs. However, a larger number of Au particles with larger sizes were deposited on the transition metal ditellurides (1T′-$MoTe_2$, WTe_2) than the disulfides (1T-WS_2, 2H-WS_2) and diselenides (2H-$MoSe_2$, 2H-WSe_2) under the same conditions (Fig. 7). This suggests that 1T′-$MoTe_2$ and WTe_2 possess stronger electron donation capabilities that are

attributed to their higher Fermi levels and semi-metallic nature relative to the disulfides and diselenides, based on the calculated band structures.

Interestingly, the deposition of Ag on the colloidal TMD nanosheets is different than Au. Ag deposits as nanoparticles on the disulfides and diselenides, but the higher surface mobility of Ag atoms results in their coalescence to form larger Ag particles. The result is a bimodal distribution of small and large Ag nanoparticles on 1T-WS_2, 2H-WS_2, 2H-$MoSe_2$, and 2H-WSe_2, which is distinct from the behavior of Au, where uniform nanoparticles are formed. On 1T′-$MoTe_2$ and WTe_2, however, Ag deposition produces a unique 2D–2D heterostructure, with atomically thin Ag layers being interfaced with the underlying basal planes of the ditellurides, as highlighted in Fig. 8a. Spectroscopic evidence corroborates the formation of interfacial Ag–Te bonds with Ag carrying a partial positive charge, and therefore the self-limiting growth of a single atomic layer of Ag on the ditellurides, which is in contrast to the deposition of zero-valent Au nanoparticles.

We sought to understand this behavior, where a 2D metal forms spontaneously on a 2D TMD substrate. We estimated the formation energy of Au and Ag clusters situated on TMD monolayers using DFT calculations and found that neither low-coverage cluster adsorbates nor high-coverage metal layers are thermodynamically favorable, pointing to kinetic factors that lead to the unique deposition behavior. A lower kinetic barrier for the deposition of Ag relative to Au at the initial nucleation stage, as revealed by theoretical calculations, facilitates much faster deposition of atomic Ag compared with the deposition of atomic Au under the same conditions (Fig. 8b). Therefore, Ag preferentially forms 2D atomic layers, facilitated by the formation of strong interfacial Ag–Te bonds. In contrast, Au tends to follow the typical heterogeneous seeded growth pathway, where adsorption of pre-existing Au nuclei form Au–Au bonds, which ultimately give rise to nanoparticles. The high density of atomic defects in the colloidal TMD nanosheets, as mentioned above, facilitate the growth of metal nanoparticles by providing the necessary nucleation sites. The formation of atomically thin Ag layers on 1T′-$MoTe_2$ and WTe_2 is less influenced by the defect density, or even slightly inhibited, as the Fermi levels of the ditellurides are slightly lowered when atomic metal or chalcogen defects are introduced. Calculation results also indicate that the charge transfer from an adsorbed Ag atom to 1T′-$MoTe_2$ (~0.116 electrons) is much larger than that from an adsorbed Au atom (~0.006 electrons), which is consistent with the spectroscopic data. Accordingly, the as-formed Ag/1T′-$MoTe_2$ prevents the Ag^+ cations from approaching the Ag atomic layer, as both are positively charged. The ability to access a variety of 0D–2D and 2D–2D heterostructures of noble metals and TMDs, and understand how such unique nanostructures form, is important for applications that depend on the noble metal/TMD interface. These applications include single-atom catalysts, where activity and selectivity can be tuned via metal–support interactions, and atomic-level engineering of electrical contacts, which function best with low chemical disorder and lowered resistance at the interface.

In addition to noble metals, colloidal TMDs have also been coupled to other non-layered chalcogenide systems to access different mixed-dimensional heterostructures with expanded functionalities. Epitaxial seeded growth, where the lattice mismatch between the two components is minimal along one direction, becomes an effective strategy for rationally designing heterostructures with well-defined atomic interfaces. Chen *et al.* reported the seed-mediated directional growth of 2D $MoSe_2$ nanosheets on the edges of one-dimensional $Cu_{2-x}S$ nanowires.[55] In the $Cu_{2-x}S$–$MoSe_2$ heterostructures, the sandwich layers of $MoSe_2$ are positioned right between the bilayer copper atoms across the interface, which is promoted by the well-matched lattice fringes of $MoSe_2$ and chalcocite Cu_2S (Fig. 8c–e). This approach can be further extended to the construction of $Cu_{2-x}S$–MoS_2 heterostructures with a similar edge

epitaxy relationship at the $Cu_{2-x}S/MoS_2$ interface. The $Cu_{2-x}S$ can then be converted to CdS using cation exchange, producing $CdS–MoS_2$ hybrids for photocatalytic HER.

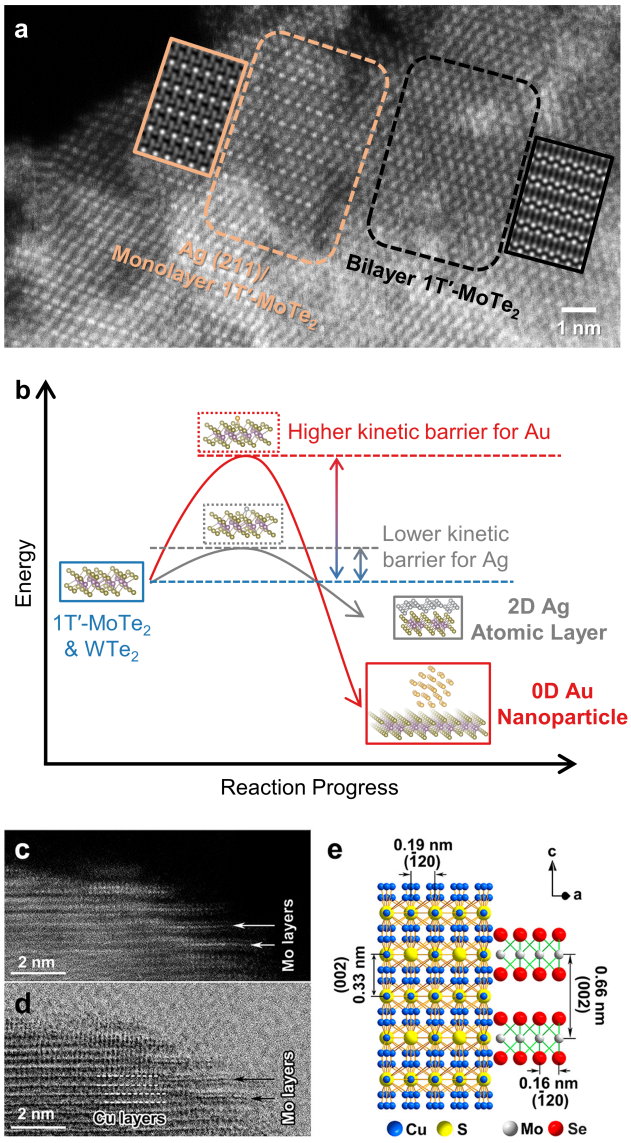

Figure 8. (a) Atomic-resolution ADF-STEM image of $Ag_{5\%}/1T′\text{-}MoTe_2$ (5% of Ag deposited on $1T′\text{-}MoTe_2$). Ag (211) planes deposited epitaxially on monolayer $1T′\text{-}MoTe_2$ and bilayer $1T′\text{-}MoTe_2$ are highlighted with dashed orange and black boxes, respectively, and the corresponding simulated ADF-STEM patterns are shown in solid orange and black boxes for comparison. (b) Schematic showing the deposition process for Au and Ag on $1T′\text{-}MoTe_2$, where the kinetic barrier during the single-atom nucleation step determines the final morphology. (a) and (b) were adapted with permission from ref. 4. Copyright 2020 Nature Publishing Group. (c) HAADF-STEM and (d) ABF-STEM images of $Cu_{2-x}S–MoSe_2$ heterostructures, together with (e) the corresponding schematic showing the epitaxial relationship between the $Cu_{2-x}S$ (002) planes and the $MoSe_2$ (002) planes. (c–e) were adapted with permission from ref. 55. Copyright 2017 American Chemical Society.

6. CONCLUSIONS AND OUTLOOK

Mono- or few-layer TMD nanosheets exhibit properties that are distinct from their bulk counterparts. During the past few years, general synthetic protocols to access colloidal TMD nanostructures have been developed, and these have considerably expanded the library of available colloidal nanocrystal systems.[1,2,14,21,50,56] These synthetic methods have expanded the scope of TMDs beyond bulk materials and substrate-bound films and nanosheets, opening the door to new applications that exploit their colloidal dispersibility, such as biomedical imaging and therapeutic applications, and high surface areas, such as catalysis and energy storage. The unique few-layer architecture of colloidal TMDs also provides a useful platform for gaining new fundamental understanding of structure, elemental distribution, crystallinity, defects, grain boundaries, and chemical reactivity in these important systems, which is useful for accessing precise nanostructural features, discovering new properties, and integrating them with other materials.

These colloidal TMD systems are also ideal platforms for further synthetic manipulation to yield more advanced nanostructures. Opportunities exist to begin targeting solution-phase modifications including doping,[57] cation and anion exchange,[58,59] intercalation and exfoliation,[35,60] interlayer coupling and decoupling,[61] interphase engineering,[36] and surface functionalization.[62,63] Such capabilities, enabled by colloidal nanochemistry, could produce precisely-defined nanostructures in a predictive manner. For example, the in-plane TMD heterostructures enabled by partial ion exchange and the vertical TMD heterostructures enabled by seeded growth could be combined to produce unique interfaced systems that would be useful for optoelectronic devices and tandem catalysts. Layer-by-layer assembly and subsequent coupling of two TMD monolayers, which would require additional advances in ligand functionalization, could also allow the construction of three-dimensional superstructures with alternating two-dimensional layers.[64] We anticipate that advances in colloidal nanochemistry will enable the design and synthesis of complex TMD nanostructures and further expand their functionalities into new multidisciplinary fields.

BIOGRAPHIES

Yifan Sun received his B.S. in chemistry from Fudan University, China in 2013. Then he went to Penn State where he worked with Raymond E. Schaak and Mauricio Terrones studying colloidal nanostructures of transition metal dichalcogenides and obtained his Ph.D. in chemistry in 2018. He is currently a postdoctoral research associate working with Sheng Dai at Oak Ridge National Laboratory, focusing on novel materials for heterogeneous catalysis.

Mauricio Terrones received his B.S. in Engineering Physics from Universidad Iberoamericana (Mexico) and Ph.D. in Chemical Physics from Sussex University under the supervision of Harold W. Kroto (FRS, Nobel Laureate). He then carried out postdocs in the UK and in Germany (Max Planck Institute fuer Metallforshcung). He returned to Mexico as a faculty at UNAM and IPICYT before moving to Penn State. He is currently the Verne M. Willaman Professor of Physics and the Director of the IUCRC-NSF Center for Atomically Thin Multifunctional Coatings (ATOMIC).

Raymond E. Schaak received his B.S. in chemistry from Lebanon Valley College and his Ph.D. in chemistry from Penn State. After a postdoc at Princeton, he joined the chemistry faculty at Texas A&M. He is currently the DuPont Professor of Materials Chemistry at Penn State and has a courtesy appointment in Chemical Engineering. His research interests focus on synthetic inorganic nanochemistry, solid-state chemistry, and new materials discovery.

ACKNOWLEDGMENTS

Y.S. and R.E.S. were supported by the U.S. National Science Foundation Grant No. CHE-1707830. M.T. acknowledges support from the Air Force Office of Scientific Research (AFOSR) Grant FA9550-18-1-0072.

REFERENCES

(1) Sun, Y.; Wang, Y.; Sun, D.; Carvalho, B. R.; Read, C. G.; Lee, C.; Lin, Z.; Fujisawa, K.; Robinson, J. A.; Crespi, V. H.; Terrones, M.; Schaak, R. E. Low-Temperature Solution Synthesis of Few-Layer 1T′-$MoTe_2$ Nanostructures Exhibiting Lattice Compression. *Angew. Chem. Int. Ed.* **2016**, *55*, 2830–2834.

(2) Sun, Y.; Fujisawa, K.; Lin, Z.; Lei, Y.; Mondschein, J. S.; Terrones, M.; Schaak, R. E. Low-Temperature Solution Synthesis of Transition Metal Dichalcogenide Alloys with Tunable Optical Properties. *J. Am. Chem. Soc.* **2017**, *139*, 11096–11105.

(3) Sun, Y.; Darling, A. J.; Li, Y.; Fujisawa, K.; Holder, C. F.; Liu, H.; Janik, M. J.; Terrones, M.; Schaak, R. E. Defect-Mediated Selective Hydrogenation of Nitroarenes on Nanostructured WS_2. *Chem. Sci.* **2019**, *10*, 10310–10317.

(4) Sun, Y.; Wang, Y.; Chen, J. Y. C.; Fujisawa, K.; Holder, C. F.; Miller, J. T.; Crespi, V. H.; Terrones, M.; Schaak, R. E. Interface-Mediated Noble Metal Deposition on Transition Metal Dichalcogenide Nanostructures. *Nat. Chem.* **2020**, *12*, 284–293.

(5) Chhowalla, M.; Shin, H. S.; Eda, G.; Li, L.-J.; Loh, K. P.; Zhang, H. The Chemistry of Two-Dimensional Layered Transition Metal Dichalcogenide Nanosheets. *Nat. Chem.* **2013**, *5*, 263–275.

(6) Lv, R.; Robinson, J. A.; Schaak, R. E.; Sun, D.; Sun, Y.; Mallouk, T. E.; Terrones, M. Transition Metal Dichalcogenides and Beyond: Synthesis, Properties, and Applications of Single- and Few-Layer Nanosheets. *Acc. Chem. Res.* **2015**, *48*, 56–64.

(7) Wang, Q. H.; Kalantar-Zadeh, K.; Kis, A.; Coleman, J. N.; Strano, M. S. Electronics and Optoelectronics of Two-Dimensional Transition Metal Dichalcogenides. *Nat. Nanotechnol.* **2012**, *7*, 699–712.

(8) Manzeli, S.; Ovchinnikov, D.; Pasquier, D.; Yazyev, O. V.; Kis, A. 2D Transition Metal Dichalcogenides. *Nat. Rev. Mater.* **2017**, *2*, 17033.

(9) Tan, C.; Cao, X.; Wu, X. J.; He, Q.; Yang, J.; Zhang, X.; Chen, J.; Zhao, W.; Han, S.; Nam, G.-H.; Sindoro, M.; Zhang, H. Recent Advances in Ultrathin Two-Dimensional Nanomaterials. *Chem. Rev.* **2017**, *117*, 6225–6331.

(10) Han, J. H.; Kwak, M.; Kim, Y.; Cheon, J. Recent Advances in the Solution-Based Preparation of Two- Dimensional Layered Transition Metal Chalcogenide Nanostructures. *Chem. Rev.* **2018**, *118*, 6151–6188.

(11) Soo Choi, H.; Liu, W.; Misra, P.; Tanaka, E.; Zimmer, J. P.; Itty Ipe, B.; Bawendi, M. G.; Frangioni, J. V. Renal Clearance of Quantum Dots. *Nat. Biotechnol.* **2007**, *25*, 1165–1170.

(12) Cargnello, M. Colloidal Nanocrystals as Building Blocks for Well-Defined Heterogeneous Catalysts. *Chem. Mater.* **2019**, *31*, 576–596.

(13) Jin, H.; Baek, B.; Kim, D.; Wu, F.; Batteas, J. D.; Cheon, J.; Son, D. H. Effects of Direct Solvent-Quantum Dot Interaction on the Optical Properties of Colloidal Monolayer WS_2 Quantum Dots. *Nano Lett.* **2017**, *17*, 7471–7477.

(14) Yoo, D.; Kim, M.; Jeong, S.; Han, J.; Cheon, J. Chemical Synthetic Strategy for Single-Layer Transition-Metal Chalcogenides. *J. Am. Chem. Soc.* **2014**, *136*, 14670–14673.

(15) Meza, E.; Diaz, R. E.; Li, C. W. Solution-Phase Activation and Functionalization of Colloidal WS_2 Nanosheets with Ni Single Atoms. *ACS Nano* **2020**, *14*, 2238–2247.
(16) Sun, D.; Feng, S.; Terrones, M.; Schaak, R. E. Formation and Interlayer Decoupling of Colloidal $MoSe_2$ Nanoflowers. *Chem. Mater.* **2015**, *27*, 3167–3175.
(17) Zhou, J.; Lin, J.; Huang, X.; Zhou, Y.; Chen, Y.; Xia, J.; Wang, H.; Xie, Y.; Yu, H.; Lei, J.; Wu, D.; Liu, F.; Fu, Q.; Zeng, Q.; Hsu, C.-H.; Yang, C.; Lu, L.; Yu, T.; Shen, Z.; Lin. H.; Yakobson, B. I.; Liu, Q.; Suenaga, K.; Liu, G.; Liu, Z. A Library of Atomically Thin Metal Chalcogenides. *Nature* **2018**, *556*, 355–359.
(18) Sokolikova, M. S.; Mattevi, C. Direct Synthesis of Metastable Phases of 2D Transition Metal Dichalcogenides. *Chem. Soc. Rev.* **2020**, *49*, 3952–3980.
(19) Uozumi, Y.; Ichii, S. Selective Hydrogenation of Nitroarenes Catalyzed by Nanostructured Tungsten Disulfide. *Synfacts* **2020**, *16*, 0193.
(20) Lin, Y.-C.; Nakajima, H.; Tseng, C.-W.; Li, S.; Liu, Z.; Okazaki, T.; Chiu, P.-W.; Suenaga, K. Does the Metallic 1T Phase WS_2 Really Exist? **2019**, arXiv:1907.11398 [cond-mat.mtrl-sci].
(21) Mahler, B.; Hoepfner, V.; Liao, K.; Ozin, G. A. Colloidal Synthesis of 1T-WS_2 and 2H-WS_2 Nanosheets: Applications for Photocatalytic Hydrogen Evolution. *J. Am. Chem. Soc.* **2014**, *136*, 14121–14127.
(22) Voiry, D.; Yamaguchi, H.; Li, J.; Silva, R.; Alves, D. C. B.; Fujita, T.; Chen, M.; Asefa, T.; Shenoy, V. B.; Eda, G.; Chhowalla, M. Enhanced Catalytic Activity in Strained Chemically Exfoliated WS_2 Nanosheets for Hydrogen Evolution. *Nat. Mater.* **2013**, *12*, 850–855.
(23) Acerce, M.; Voiry, D.; Chhowalla, M. Metallic 1T Phase MoS_2 Nanosheets as Supercapacitor Electrode Materials. *Nat. Nanotechnol.* **2015**, *10*, 313–318.
(24) Qi, Y.; Naumov, P. G.; Ali, M. N.; Rajamathi, C. R.; Schnelle, W.; Barkalov, O.; Hanfland, M.; Wu, S.-C.; Shekhar, C.; Sun, Y.; Süß, V.; Schmidt, M.; Schwarz, U.; Pippel, E.; Werner, P.; Hillebrand, R.; Förster, T.; Kampert, E.; Parkin, S.; Cava, R. J.; Felser, C.; Yan, B.; Medvedev, S. A. Superconductivity in Weyl Semimetal Candidate $MoTe_2$. *Nat. Commun.* **2016**, *7*, 11038.
(25) Yu, Y.; Nam, G.-H.; He, Q.; Wu, X.-J.; Zhang, K.; Yang, Z.; Chen, J.; Ma, Q.; Zhao, M.; Liu, Z.; Ran, F.-R.; Wang, X.; Li, H.; Huang, X.; Li, B.; Xiong, Q.; Zhang, Q.; Liu, Z.; Gu, L.; Du, Y.; Huang, W.; Zhang, H. High Phase-Purity 1T′-MoS_2- and 1T′-$MoSe_2$-Layered Crystals. *Nat. Chem.* **2018**, *10*, 638–643.
(26) Vaughn, D. D.; Patel, R. J.; Hickner, M. A.; Schaak, R. E. Single-Crystal Colloidal Nanosheets of GeS and GeSe. *J. Am. Chem. Soc.* **2010**, *132*, 15170–15172.
(27) Sokolikova, M. S.; Sherrell, P. C.; Palczynski, P.; Bemmer, V. L.; Mattevi, C. Direct Solution-Phase Synthesis of 1T′ WSe_2 Nanosheets. *Nat. Commun.* **2019**, *10*, 712.
(28) Keum, D. H.; Cho, S.; Kim, J. H.; Choe, D.-H.; Sung, H.-J.; Kan, M.; Kang, H.; Hwang, J.-Y.; Kim, S. W.; Yang, H.; Chang, K. J. Lee, Y. H. Bandgap Opening in Few-Layered Monoclinic $MoTe_2$. *Nat. Phys.* **2015**, *11*, 482–486.
(29) Cho, S.; Kim, S.; Kim, J. H.; Zhao, J.; Seok, J.; Keum, D. H.; Baik, J.; Choe, D.-H.; Chang, K. J.; Suenaga, K.; Kim, S. W.; Lee, Y. H. Yang, H. Phase Patterning for Ohmic Homojunction Contact in $MoTe_2$. *Science* **2015**, *349*, 625–628.
(30) Ali, M. N.; Xiong, J.; Flynn, S.; Tao, J.; Gibson, Q. D.; Schoop, L. M.; Liang, T.; Haldolaarachchige, N.; Hirschberger, M.; Ong, N. P.; Cava, R. J. Large, Non-Saturating Magnetoresistance in WTe_2. *Nature* **2014**, *514*, 205–208.
(31) Sines, I. T.; Vaughn, D. D.; Biacchi, A. J.; Kingsley, C. E.; Popczun, E. J.; Schaak, R. E. Engineering Porosity into Single-Crystal Colloidal Nanosheets Using Epitaxial Nucleation and Chalcogenide Anion Exchange Reactions: The Conversion of SnSe to SnTe. *Chem. Mater.* **2012**, *24*, 3088–3093.
(32) Mourdikoudis, S.; Liz-Marzán, L. M. Oleylamine in Nanoparticle Synthesis. *Chem. Mater.* **2013**, *25*, 1465–1476.

(33) Sun, Y.; Fujisawa, K.; Terrones, M.; Schaak, R. E. Solution Synthesis of Few-Layer WTe_2 and $Mo_xW_{1-x}Te_2$ Nanostructures. *J. Mater. Chem. C* **2017**, *5*, 11317–11323.
(34) Zhou, J.; Liu, F.; Lin, J.; Huang, X.; Xia, J.; Zhang, B.; Zeng, Q.; Wang, H.; Zhu, C.; Niu, L.; Wang, X.; Fu, W.; Yu, P.; Chang, T.-R.; Hsu, C.-H.; Wu, D.; Jeng, H.-T.; Huang, Y.; Lin, H.; Shen, Z.; Yang, C.; Lu, L.; Suenaga, K.; Zhou, W.; Pantelides, S. T.; Liu, G.; Liu, Z. Large-Area and High-Quality 2D Transition Metal Telluride. *Adv. Mater.* **2017**, *29*, 1603471.
(35) Fan, X.; Xu, P.; Zhou, D.; Sun, Y.; Li, Y. C.; Nguyen, M. A. T.; Terrones, M.; Mallouk, T. E. Fast and Efficient Preparation of Exfoliated 2H MoS_2 Nanosheets by Sonication-Assisted Lithium Intercalation and Infrared Laser-Induced 1T to 2H Phase Reversion. *Nano Lett.* **2015**, *15*, 5956–5960.
(36) Chou, S. S.; De, M.; Kim, J.; Byun, S.; Dykstra, C.; Yu, J.; Huang, J.; Dravid, V. P. Ligand Conjugation of Chemically Exfoliated MoS_2. *J. Am. Chem. Soc.* **2013**, *135*, 4584–4587.
(37) Son, D.; Chae, S. I.; Kim, M.; Choi, M. K.; Yang, J.; Park, K.; Kale, V. S.; Koo, J. H.; Choi, C.; Lee, M.; Kim, J. H.; Hyeon, T.; Kim, D.-H. Colloidal Synthesis of Uniform-Sized Molybdenum Disulfide Nanosheets for Wafer-Scale Flexible Nonvolatile Memory. *Adv. Mater.* **2016**, *28*, 9326–9332.
(38) Zeng, Q.; Wang, H.; Fu, W.; Gong, Y.; Zhou, W.; Ajayan, P. M.; Lou, J.; Liu, Z. Band Engineering for Novel Two-Dimensional Atomic Layers. *Small* **2015**, *11*, 1868–1884.
(39) Holder, C. F.; Schaak, R. E. Tutorial on Powder X-Ray Diffraction for Characterizing Nanoscale Materials. *ACS Nano* **2019**, *13*, 7359–7365.
(40) Zhao, X.; Ning, S.; Fu, W.; Pennycook, S. J.; Loh, K. P. Differentiating Polymorphs in Molybdenum Disulfide via Electron Microscopy. *Adv. Mater.* **2018**, *30*, 1802397.
(41) Tan, T. L.; Ng, M.-F.; Eda, G. Stable Monolayer Transition Metal Dichalcogenide Ordered Alloys with Tunable Electronic Properties. *J. Phys. Chem. C* **2016**, *120*, 2501–2508.
(42) Lin, Z.; Carvalho, B. R.; Kahn, E.; Lv, R.; Rao, R.; Terrones, H.; Pimenta, M. A.; Terrones, M. Defect Engineering of Two-Dimensional Transition Metal Dichalcogenides. *2D Mater.* **2016**, *3*, 022002.
(43) Zhang, F.; Lu, Y.; Schulman, D. S.; Zhang, T.; Fujisawa, K.; Lin, Z.; Lei, Y.; Elias, A. L.; Das, S.; Sinnott, S. B.; Terrones, M. Carbon Doping of WS_2 Monolayers: Bandgap Reduction and p-Type Doping Transport. *Sci. Adv.* **2019**, *5*, eaav5003.
(44) Schmidt, H.; Giustiniano, F.; Eda, G. Electronic Transport Properties of Transition Metal Dichalcogenide Field-Effect Devices: Surface and Interface Effects. *Chem. Soc. Rev.* **2015**, *44*, 7715–7736.
(45) Li, H.; Tsai, C.; Koh, A. L.; Cai, L.; Contryman, A. W.; Fragapane, A. H.; Zhao, J.; Han, H. S.; Manoharan, H. C.; Abild-Pedersen, F.; Nørskov, J. K.; Zheng, X. Activating and Optimizing MoS_2 Basal Planes for Hydrogen Evolution through the Formation of Strained Sulphur Vacancies. *Nat. Mater.* **2016**, *15*, 48–53.
(46) Hinnemann, B.; Moses, P. G.; Bonde, J.; Jørgensen, K. P.; Nielsen, J. H.; Horch, S.; Chorkendorff, I.; Nørskov, J. K. Biomimetic Hydrogen Evolution: MoS_2 Nanoparticles as Catalyst for Hydrogen Evolution. *J. Am. Chem. Soc.* **2005**, *127*, 5308–5309.
(47) Voorhoeve, R. J. H. Electron Spin Resonance Study of Active Centers in Nickel-Tungsten Sulfide Hydrogenation Catalysts. *J. Catal.* **1971**, *23*, 236–242.
(48) Sorribes, I.; Liu, L.; Corma, A. Nanolayered Co–Mo–S Catalysts for the Chemoselective Hydrogenation of Nitroarenes. *ACS Catal.* **2017**, *7*, 2698–2708.
(49) Lei, Y.; Butler, D.; Lucking, M. C.; Zhang, F.; Xia, T.; Fujisawa, K.; Granzier-Nakajima, T.; Cruz-Silva, R.; Endo, M.; Terrones, H.; Terrones, M.; Ebrahimi, A. Single-Atom Doping of MoS_2 with Manganese Enables Ultrasensitive Detection of Dopamine: Experimental and Computational Approach. *Sci. Adv.* **2020**, *6*, eabc4250.
(50) Han, J. H.; Kim, H. K.; Baek, B.; Han, J.; Ahn, H. S.; Baik, M.; Cheon, J. Activation of the Basal Plane in Two Dimensional Transition Metal Chalcogenide Nanostructures. *J. Am.*

Chem. Soc. **2018**, *140*, 13663–13671.
(51) Jin, H.; Ahn, M.; Jeong, S.; Han, J. H.; Yoo, D.; Son, D. H.; Cheon, J. Colloidal Single-Layer Quantum Dots with Lateral Confinement Effects on 2D Exciton. *J. Am. Chem. Soc.* **2016**, *138*, 13253–13259.
(52) Zhang, F.; Zheng, W.; Lu, Y.; Pabbi, L.; Fujisawa, K.; Elías, A. L.; Binion, A. R.; Granzier-Nakajima, T.; Zhang, T.; Lei, Y.; Lin, Z.; Hudson, E. W.; Sinnott, S. B.; Balicas, L.; Terrones, M. Superconductivity Enhancement in Phase-Engineered Molybdenum Carbide/Disulfide Vertical Heterostructures. *Proc. Natl. Acad. Sci. U.S.A.* **2020**, *117*, 19685–19693.
(53) Huang, X.; Zeng, Z.; Bao, S.; Wang, M.; Qi, X.; Fan, Z.; Zhang, H. Solution-Phase Epitaxial Growth of Noble Metal Nanostructures on Dispersible Single-Layer Molybdenum Disulfide Nanosheets. *Nat. Commun.* **2013**, *4*, 1444.
(54) Liu, Y.; Guo, J.; Zhu, E.; Liao, L.; Lee, S.; Ding, M.; Shakir, I.; Gambin, V.; Huang, Y.; Duan, X. Approaching the Schottky–Mott Limit in van Der Waals Metal–Semiconductor Junctions. *Nature* **2018**, *557*, 696–700.
(55) Chen, J.; Wu, X. J.; Gong, Y.; Zhu, Y.; Yang, Z.; Li, B.; Lu, Q.; Yu, Y.; Han, S.; Zhang, Z.; Zong, Y.; Han, Y.; Gu, L.; Zhang, H. Edge Epitaxy of Two-Dimensional $MoSe_2$ and MoS_2 Nanosheets on One-Dimensional Nanowires. *J. Am. Chem. Soc.* **2017**, *139*, 8653–8660.
(56) Jeong, S.; Yoo, D.; Jang, J.; Kim, M.; Cheon, J. Well-Defined Colloidal 2-D Layered Transition-Metal Chalcogenide Nanocrystals via Generalized Synthetic Protocols. *J. Am. Chem. Soc.* **2012**, *134*, 18233–18236.
(57) Shi, Y.; Zhou, Y.; Yang, D.-R.; Xu, W.-X.; Wang, C.; Wang, F.-B.; Xu, J.-J.; Xia, X.-H.; Chen, H.-Y. Energy Level Engineering of MoS_2 by Transition-Metal Doping for Accelerating Hydrogen Evolution Reaction. *J. Am. Chem. Soc.* **2017**, *139*, 15479–15485.
(58) Hodges, J. M.; Kletetschka, K.; Fenton, J. L.; Read, C. G.; Schaak, R. E. Sequential Anion and Cation Exchange Reactions for Complete Material Transformations of Nanoparticles with Morphological Retention. *Angew. Chem. Int. Ed.* **2015**, *54*, 8669–8672.
(59) Schaak, R. E.; Steimle, B. C.; Fenton, J. L. Made-to-Order Heterostructured Nanoparticle Libraries. *Acc. Chem. Res.* **2020**, *53*, 2558–2568.
(60) Koski, K. J.; Wessells, C. D.; Reed, B. W.; Cha, J. J.; Kong, D.; Cui, Y. Chemical Intercalation of Zerovalent Metals into 2D Layered Bi_2Se_3 Nanoribbons. *J. Am. Chem. Soc.* **2012**, *134*, 13773–13779.
(61) Kempt, R.; Kuc, A.; Han, J. H.; Cheon, J.; Heine, T. 2D Crystals in Three Dimensions: Electronic Decoupling of Single-Layered Platelets in Colloidal Nanoparticles. *Small* **2018**, *14*, 1803910.
(62) Voiry, D.; Goswami, A.; Kappera, R.; de Carvalho Castro e Silva, C.; Kaplan, D.; Fujita, T.; Chen, M.; Asefa, T.; Chhowalla, M. Covalent Functionalization of Monolayered Transition Metal Dichalcogenides by Phase Engineering. *Nat. Chem.* **2015**, *7*, 45–49.
(63) Liu, H.; Grasseschi, D.; Dodda, A.; Fujisawa, K.; Olson, D.; Kahn, E.; Zhang, F.; Zhang, T.; Lei, Y.; Branco, R. B. N.; Elías, A. L.; Silva, R. C.; Yeh, Y.-T.; Maroneze, C. M.; Seixas, L.; Hopkins, P.; Das, S.; de Matos, C. J. S.; Terrones, M. Spontaneous Chemical Functionalization via Coordination of Au Single Atoms on Monolayer MoS_2. *Sci. Adv.* **2020**, *6*, eabc9308.
(64) Liu, Y.; Siron, M.; Lu, D.; Yang, J.; dos Reis, R.; Cui, F.; Gao, M.; Lai, M.; Lin, J.; Kong, Q.; Lei, T.; Kang, J.; Jin, J.; Ciston, J.; Yang, P. Self-Assembly of Two-Dimensional Perovskite Nanosheet Building Blocks into Ordered Ruddlesden–Popper Perovskite Phase. *J. Am. Chem. Soc.* **2019**, *141*, 13028–13032.

Table of Contents Graphic